analytical chemistry

pubs.acs.org/ac Article

A Dopamine-Enabled Universal Assay for Catalase and Catalase-Like Nanozymes

Anqi Lin, Quanyi Liu, Yihong Zhang, Quan Wang, Sirong Li, Bijun Zhu, Leiying Miao, Yan Du, Sheng Zhao,* and Hui Wei*

Cite This: *Anal. Chem.* 2022, 94, 10636−10642 Read Online

ACCESS | Metrics & More | Article Recommendations | Supporting Information

ABSTRACT: Developing a universal strategy to measure catalase (CAT)/CAT-like activity, on one hand, overcomes limitations on current assays, such as moderate sensitivity and limited sample scope; on the other hand, facilitates insightful studies on applications of CAT and CAT-like nanozymes. Herein, the oxygen-sensitive and H_2O_2-inhibitory self-polymerization of dopamine (DA) was demonstrated as an activity indicator of CAT or CAT-like nanozymes, which monitors the catalytically generated O_2 in a hypoxic environment. A typical assay for natural CAT was achieved under the optimized conditions. Moreover, this assay was suitable for diverse types of samples, ranging from nanozymes, animal tissues, to human saliva. By comparing the merits and limitations of common methods, this assay shows all-round advantages in sensitivity, specificity, and versatility, facilitating the formulation of measurement criteria and the development of potential standardized assays for CAT (or CAT-like nanozyme) activity.

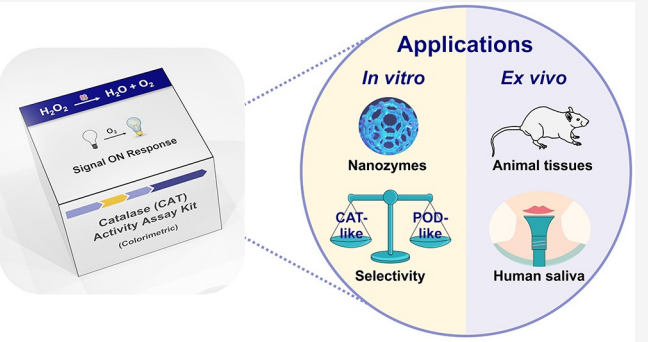

Catalase (CAT), which converts hydrogen peroxide (H_2O_2) to molecular oxygen and water, is ubiquitously present in the peroxisomes of all aerobic organisms (*i.e.*, microorganisms, animals, and plants).[1,2] As a key component of the antioxidant defense system in cells, CAT acts as a biomarker to track the pathological status of many diseases as well as drug-induced toxicity.[3−5] Aside from natural CAT, CAT-like nanozymes have attracted considerable interest in biological applications because of their high stability, low cost, and ease of preparation.[6−10] Recently, numerous nanozymes with high CAT-like activity have been employed to treat oxidative stress-related diseases.[11−14] Thus, the determination of CAT (or CAT-like nanozyme) activity is essential not only for precise assessment of physiological and pathological conditions in organisms but also for rational design of CAT mimics with high efficiency.

To date, two types of strategies have been employed to measure the activity of CAT and CAT-like nanozymes: the determination of residual H_2O_2 and the detection of generated O_2. The determination of residual H_2O_2 is mostly employed because of its ease of implementation. Therein, the spectrophotometric assay based on the absorbance of H_2O_2 at 240 nm and horseradish peroxidase (HRP)-based colorimetric or fluorometric assays are the most widely used.[2,15] However, they are inevitably associated with some disadvantages. First, the limited sensitivity of the spectrophotometric assay (due to the low molar extinction coefficient of H_2O_2) has hindered the usage of the assay when H_2O_2 was at physiological and nontoxic levels (usually in the micromolar range).[2] Additionally, it is not suitable for samples with a strong absorbance at 240 nm, for example, for some CAT-like nanozymes, turbid cell suspensions, and tissue homogenates.[3] Moreover, other H_2O_2-involved non-CAT-catalyzed pathways may also lead to false-positive results when using HRP-based assays, making not applicable for many nanozymes with simultaneous CAT- and peroxidase (POD)-like activities. Likewise, H_2O_2-specific dyes also meet the dilemma of sophisticated fabrication and ability to anti-interference.[16]

Therefore, the activity of CAT (or CAT-like nanozymes) can be more accurately measured via the detection of generated O_2. The dissolved oxygen electrode and optical sensor are most commonly used to measure the generated O_2 because of their accuracy. Nevertheless, they have several limitations for practical use. First, homogeneous sample solutions are needed. Second, the dynamic range is narrow because of the saturated concentration of dissolved oxygen, which leads to the inaccuracy of highly active CAT or CAT-like nanozymes. Additionally, it is not applicable to high-

Received: February 17, 2022
Accepted: June 9, 2022
Published: June 27, 2022

https://doi.org/10.1021/acs.analchem.2c00804
Anal. Chem. 2022, 94, 10636−10642

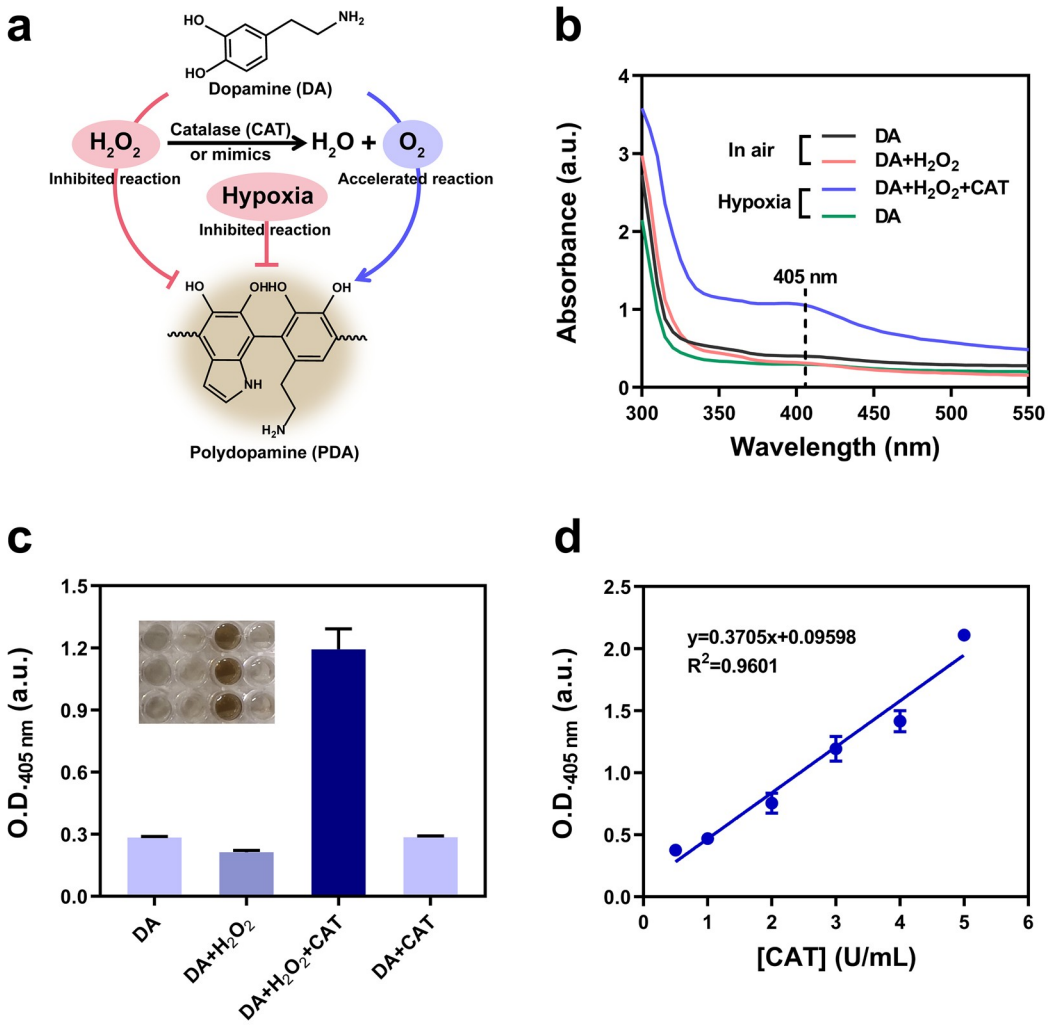

Figure 1. Sensing mechanism and typical assay for natural CAT. (a) Schematic illustration of CAT (or CAT mimics)-enhanced DA self-polymerization in a hypoxic environment. (b) UV−vis absorption spectrum of DA polymerization when treated under different conditions. (c) Quantitative bar chart of the DA-enabled assay for CAT (from *Aspergillus niger*). Inset: digital photograph of the assay solutions in a well plate in the indicated groups. (d) Linear correlation between the $O.D._{405\ nm}$ values and the concentrations of CAT. (b−d) DA (1 mg/mL) and H_2O_2 (20 mM) were used for (b)−(d). CAT (3 U/mL) was used for (b) and (c). The reaction time was 30 min for (b)−(d). Data are expressed as mean ± standard error of the mean (n = 3) for (c) and (d). All tests were carried out at 37 °C.

throughput analysis. Recently, gas pressure assays have been explored to measure the activity of CAT (or CAT-like nanozymes).[17,18] However, complicated devices and moderate sensitivity are inevitable for these assays. To our knowledge, there are no universal methods for both CAT and CAT-like nanozymes via measuring the generated O_2. Thus, a new strategy for measuring CAT (or CAT-like nanozyme) activity is required to address the above limitations.

Herein, we demonstrated a dopamine (DA)-based universal assay to detect oxygen levels for CAT (or CAT-like) activity. DA was used as an oxygen-sensitive molecular probe. The self-polymerization of DA was markedly inhibited under hypoxic conditions or in the presence of H_2O_2. When CAT (or CAT-like nanozymes) existed in the catalytic system, DA polymerization was activated by O_2 released from the decomposition of H_2O_2. Under the optimized conditions, we achieved a typical assay for natural CAT with a concentration range of 0.5−5 U/mL. In addition to CAT, the DA-enabled assay was applicable to diverse types of samples, including CAT-like nanozymes, animal tissues, and human saliva. This assay presented all-round advantages in sensitivity, specificity, and versatility over the state-of-the-art methodologies, facilitating the formulation of measurement criteria and the development of potential standardized assays for CAT (or CAT-like nanozyme) activity.

EXPERIMENTAL SECTION

Measurement of DA-Based CAT (or CAT-Like Nanozyme) Activity. In a typical measurement, the reaction system in the 96-well plate contained 5 μL CAT (120 U/mL), 90 μL Tris buffer (10 mM, pH 8.5), 100 μL DA (2 mg/mL), and 5 μL H_2O_2 (0.8 M). After adding the solution into the plate, the plate was quickly transferred to the anaerobic device and incubated at 37 °C for 30 min. Finally, the absorbance at 405 nm was recorded by using a microplate spectrophotometer. For CAT-like nanozymes, animal tissues, and human salivary samples, CAT was replaced by diverse nanomaterials and supernatants in different tissue homogenates. For the robustness of the assay, CAT was replaced by solutions of different ions and biomolecules.

https://doi.org/10.1021/acs.analchem.2c00804
Anal. Chem. 2022, 94, 10636−10642

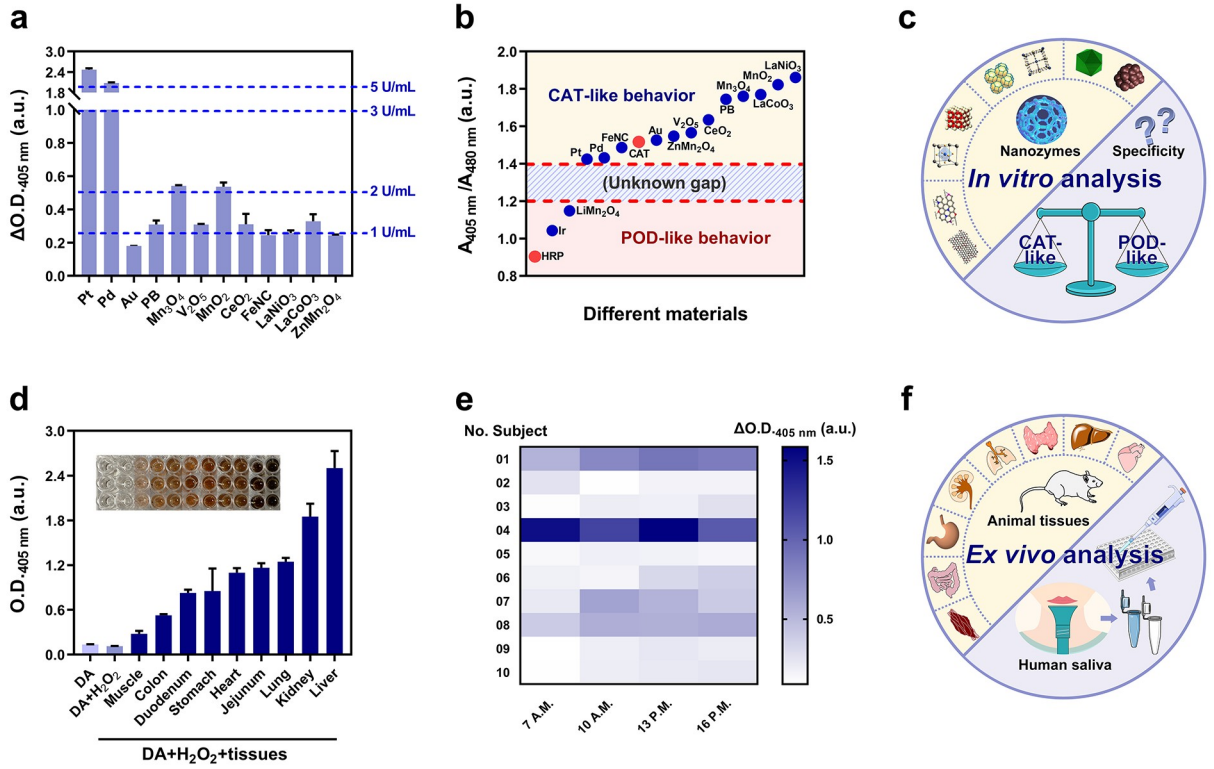

Figure 2. Versatility of the assay for nanozymes, CAT in animal tissues, and human saliva. (a) Comparison of CAT-like activity for diverse CAT-like nanozymes. (b) Classification of diverse materials including HRP, CAT, and different nanozymes based on the $A_{405\ nm}/A_{480\ nm}$ values. (c) Schematic illustration of universal *in vitro* analysis for nanozymes based on the DA-enabled assay. (d) DA-enabled assay for different tissue homogenates prepared from ICR mice. Inset: digital photograph of the assay solutions in a well plate in the indicated groups. (e) DA-enabled assay for human saliva collected at different times from healthy subjects. (f) Schematic illustration of versatile *ex vivo* analysis for animal tissues and human saliva based on the DA-enabled assay. H_2O_2 (20 mM) were used for (a)−(d). In (a), DA (1 mg/mL), Pt nanozyme (10 μg/mL), and the other nanozymes (20 μg/mL) were used. Tests of (a) were carried out at 37 °C for 30 min. In (b), the concentration of DA was 0.5 mg/mL for the HRP test and 1 mg/mL for the other tests. The concentration of material was 1 U/mL for the HRP test, 3 U/mL for the CAT test, 10 μg/mL for the Ir and Pt nanozyme tests, and 20 μg/mL for the other nanozyme tests. The reaction time was 3 min for the tests of HRP, Ir, $LiMn_2O_4$, Pt, and Pd nanozymes. The reaction time was 30 min for the other tests. (c, d) DA (1 mg/mL) was used, and all tests were carried out at 37 °C for 10 min. The results of (a) and (d) are expressed as $\Delta O.D._{\cdot 405\ nm} = x_3 - (x_4 - x_1) - x_2$, where x_1 is $O.D._{\cdot 405\ nm}$ (DA), x_2 is $O.D._{\cdot 405\ nm}$ (DA+H_2O_2), x_3 is $O.D._{\cdot 405\ nm}$ (DA+H_2O_2+sample) and x_4 is $O.D._{\cdot 405\ nm}$ (DA+sample). All data are expressed as mean ± standard error of the mean (n = 3).

Preparation of Animal Tissue Homogenates. The animal experiment was authorized by the Animal Care and Use Committee of Nanjing Drum Tower Hospital, the Affiliated Hospital of Nanjing University. After 1 week of adaptive breeding, ICR male mice (6−8 weeks) were sacrificed and the following tissues were excised. Muscle, colon, duodenum, stomach, heart, jejunum, lung, kidney, and liver were isolated from the mice, followed by the lavation of excess normal saline. Then, the tissues were cut into pieces, lysed by RIPA lysis buffer (Thermo Fisher Scientific) (10 mg tissue pieces/300 μL RIPA lysis buffer) and treated to obtain tissue homogenates. The supernatants of 10 μL in different tissue homogenates were used as sample solutions in the DA-enabled assay for CAT activity.

Saliva Collection. The experiment was authorized by the Ethics Committee of Nanjing Stomatological Hospital, the Affiliated Hospital of Nanjing University. All subjects (20−29 years old) were healthy without any systemic, infectious, or psychological diseases. They had not consumed food or beverages other than pure water for at least 90 min prior to saliva collection.

Nonstimulated whole saliva was collected from the subjects via the spitting method. In the same, quiet, and separate room, the subjects did not feel uncomfortable or upset. After 5 min of adaptation to the environment and upon rinsing the mouth thoroughly with deionized water three times, the subjects had their saliva collected in a comfortably seated position with eyes open, head tilted slightly forward, and to minimize orofacial movements. Saliva was allowed to accumulate at the bottom of the oral cavity, and the subject spat it out into a sterile test tube preplaced in a container with ice every 60 s. Saliva collected in the first minute was discarded, and the collection time was 10−15 min. After collection, saliva was immediately centrifuged (3000 *g*, 20 min, 4 °C), and butylated hydroxytoluene (BHT) (10 μL 0.5 M BHT in acetonitrile/1 mL supernatant) was added to the supernatants to prevent oxidation processes, followed by storage at −80 °C. The supernatants freely melted at 4 °C before the measurement of CAT activity. The supernatants of 10 μL were used as sample solutions in the 200 μL system for the DA-enabled assay and the spectrophotometric assay.

RESULTS AND DISCUSSION

Sensing Mechanism and Typical Assay for Natural CAT. DA, a polyphenol compound, was chosen as a molecular probe to detect oxygen levels to sense CAT activity because of its unique oxygen-sensitive and H_2O_2-inhibitory polymer-

https://doi.org/10.1021/acs.analchem.2c00804
Anal. Chem. 2022, 94, 10636−10642

ization as well as its colored product.[19,20] As shown in Figure 1a, DA aqueous solution can self-polymerize spontaneously under ambient aerobic conditions, although in a slow process. In a hypoxic environment, DA polymerization is strongly inhibited. Moreover, the presence of H_2O_2 can also inhibit polymerization even under ambient aerobic conditions, which is attributed to the reducing capacity of H_2O_2 toward the oxidized quinonoid intermediate (SI Figure S1).[21,22] Such H_2O_2-mediated inhibition can minimize the background signal from DA autoxidation for this assay. In contrast, when CAT (or CAT-like nanozyme) exists in the detection system under hypoxic conditions, it catalyzes the decomposition of H_2O_2 to generate O_2 and then accelerates DA polymerization.

As shown in Figure 1b, compared with DA under hypoxic conditions, after incubation under ambient aerobic conditions for 30 min, DA exhibited a broad absorption peak at approximately 405 nm, originating from the colored product polydopamine (PDA). The presence of H_2O_2 indeed inhibited DA autoxidation in a concentration- and reaction time-dependent manner (SI Figure S2). When CAT was present in the detection system, a more pronounced absorbance at 405 nm was observed, confirming the feasibility of this assay toward CAT (Figure 1b). This colorimetric assay could be carried out by using a UV−visible spectrophotometer or a microplate reader to measure the absorbance at 405 nm. The activity of CAT (or a CAT-like nanozyme) is positively correlated with the absorbance at 405 nm.

After the assay condition optimization (see SI Figures S3−S12, Table S1, and associated discussion), a typical assay for natural CAT from *Aspergillus niger* was carried out as an example (Figure 1c,d and SI Figure S13). As shown in Figure 1c and SI Figure S13a, the presence of both CAT and H_2O_2 resulted in a colored solution and an obvious absorbance at 405 nm. Moreover, the presence of as high as 5 U/mL CAT alone showed a negligible effect on DA polymerization because of the good specificity of CAT (SI Figure S13b). The $O.D._{405\ nm}$ showed a linear increase for CAT from 0.5 to 5 U/mL ($O.D._{405\ nm}$ = 0.09598 + 0.3705[CAT] mL/U, R^2=0.9601) (Figure 1d). Additionally, this assay presented excellent reproducibility as well (see SI Figure S14 and associated discussion).

Versatility and Specificity of the Assay for CAT-Like Nanozymes. With the increasing development of catalytic nanomaterials, especially nanozymes in bioanalysis and biomedicine, an accurate and convenient assay for CAT-like nanozymes is urgently required at the present stage. In this work, we selected 20 types of nanomaterials commonly used in the literature (13 types were synthesized while the others were commercially available). The XRD patterns and TEM images are shown in SI Figures S15 and S16, confirming the crystalline nature as well as the size and morphology of these nanomaterials. Then, the CAT-like activities of these nanomaterials were investigated by using the DA-enabled assay to assess the feasibility for nanozymes (SI Figures S17 and S18). Unlike natural CAT, however, many CAT-like nanozymes (*e.g.*, Pt, Au, Mn_3O_4, V_2O_5, and CeO_2 in this study) also exhibited oxidase (OXD)-like activities. Therefore, similar phenomena were observed among them that DA+sample exhibited an obvious increase in the $O.D._{405\ nm}$ value compared with DA (SI Figure S18). Then, we chose 12 types of tested nanomaterials with obvious CAT-like activity for standardized comparison. To establish a valid comparison of CAT-like nanozymes, we defined a $\Delta O.D._{405\ nm}$ value based on eq 1 to eliminate the contribution from the OXD-like activity of nanozymes:

$$\Delta O.D._{405\ nm} = x_3 - (x_4 - x_1) - x_2 \quad (1)$$

where x_1 is $O.D._{405\ nm}$ (DA), x_2 is $O.D._{405\ nm}$ (DA+H_2O_2), x_3 is $O.D._{405\ nm}$ (DA+H_2O_2+sample) and x_4 is $O.D._{405\ nm}$ (DA +sample). We also calculated the $\Delta O.D._{405\ nm}$ of natural CAT from the data in SI Figure S13b, which was then used as a reference standard to compare the CAT-like activities of different nanozymes. As shown in Figure 2a, both highly active nanozymes and slightly active ones could be measured under identical conditions using this assay, facilitating an objective and standardized comparison among diverse nanozymes. A concentration-dependent assay for CAT-like activity could also be achieved, taking Prussian blue (PB) as an example (SI Figure S19). The results presented a good linear correlation between $\Delta O.D._{405\ nm}$ and the concentration of PB.

In addition, DA can also act as the substrate of peroxidation incubated with H_2O_2. In general, a POD (such as HRP) catalyzes the H_2O_2-mediated peroxidation of DA to aminochrome at acidic pH, forming the brick-red product with a maximum absorbance at 480 nm (SI Figure S20a).[23] The reaction proceeds quickly. Thus, we carried out subsequent assays after incubation for 3 min. Taking HRP detection as an example, a broadened peak between 375 and 600 nm was observed (SI Figure S20b), indicating that a mixture of PDA and aminochrome formed via the catalysis of HRP at alkaline pH 8.5. The peroxidation of DA would not occur in the absence of H_2O_2 due to the good specificity of HRP.

A similar peroxidation phenomenon occurred when the assay was carried out for Ir and $LiMn_2O_4$ nanozymes. Their XRD patterns and TEM images are shown in SI Figure S21. The results indicated that Ir and $LiMn_2O_4$ tended to be POD-like in the hypoxia-DA system at alkaline pH (SI Figure S22a,b). However, nanozymes such as Pt and Pd, although with both CAT- and POD-like activities, presented CAT-dominated catalytic activity in this system (SI Figure S22c,d). This would lead to the occurrence of an obvious peak at 405 nm at the early stage of the reaction (3 min).

Thus, we defined $A_{405\ nm}/A_{480\ nm}$ as a measurement index to determine the selectivity of a CAT-/POD-like behavior for nanozymes. As shown in Figure 2b, diverse nanozymes tested above could be well classified based on the following standard. When $A_{405\ nm}/A_{480\ nm}$ was more than 1.4, the sample tended to show a CAT-like behavior. When $A_{405\ nm}/A_{480\ nm}$ was less than 1.2, the sample preferred to be POD-like. However, there was an unknown gap between the $A_{405\ nm}/A_{480\ nm}$ values of 1.2 and 1.4, which requires further studies to explain it clearly. Additionally, 3 min was recommended to measure highly active samples and 10−30 min was recommended for less active ones.

Based on the results above, we found that the DA-enabled assay was not only universal for CAT-like nanozymes, but also feasible to reveal the CAT-like/POD-like selectivity for diverse nanozymes (Figure 2c).

Detection of CAT in Animal Tissues. Next, to evaluate the feasibility of the practical applications of the DA-enabled assay, CAT in animal tissues as typical biological samples was investigated (Figure 2d and SI Figure S23). As shown in Figure 2d, the level of $O.D._{405\ nm}$ could reflect the content of CAT in different tissues, with the highest content of CAT in the liver and the lowest content in the muscle. This result was in good concordance with the literature reports.[24] Furthermore, the

https://doi.org/10.1021/acs.analchem.2c00804
Anal. Chem. 2022, 94, 10636−10642

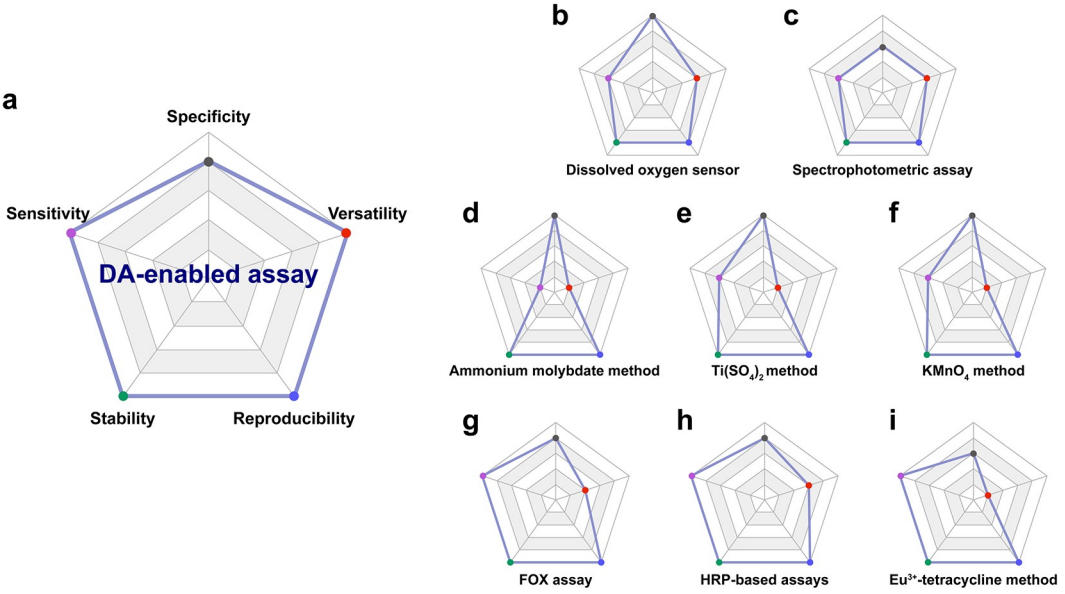

Figure 3. Comparison of methods for CAT activity assay, including the DA-enabled assay in this work (a), dissolved oxygen sensor (b), spectrophotometric assay (c), ammonium molybdate method (d), $Ti(SO_4)_2$ method (e), $KMnO_4$ method (f), FOX assay (g), HRP-based assays (h), and Eu^{3+}-tetracycline method (i).

CAT content in diluted tissue homogenates was determined. There was a good concentration-dependent correlation when using a high-content liver solution and a low-content colon solution, illustrating the excellent sensitivity and accuracy of the assay (SI Figure S23).

Detection of CAT in Human Saliva. To demonstrate the clinical and translational promise of the DA-enabled assay, CAT in human saliva was studied. We collected the nonstimulated whole saliva at different diurnal times from 10 healthy subjects. To differentially present salivary CAT activity profiling, we calculated the $\Delta O.D._{405\ nm}$ of all tested samples and summarized it as the heatmap shown in Figure 2e. The level of $\Delta O.D._{405\ nm}$ could reflect salivary CAT activity, which fluctuated with diurnal time within a reasonable range. It is worth noting that the results of Subject No. 04 at any diurnal time were comparatively higher than those of the other subjects. This was attributed to minute hemorrhages in saliva occurring in Subject No. 04, and the excess CAT from bleeding contributed to the result.[25] In fact, it was inevitable that individual differences caused large variation in total protein contents of all tested samples (SI Table S2), leading to the widely varied results of measurements. Therefore, the final relative activity was standardized to mg of total protein, and the results are shown in SI Figure S24. We found that the differences among the values were not significantly correlated with gender. Then, we investigated the performance between the DA-enabled assay and conventional spectrophotometric assay (see SI Figure S25 and associated discussion). The results indicated that this assay showed a higher sensitivity and a larger detection range, facilitating the determination of practical samples under identical conditions.

According to the results for animal tissues and human saliva, the DA-enabled assay presented excellent versatility in diverse types of samples, which was suitable for ex vivo analysis in practice (Figure 2f).

Advantages over Conventional Methods for CAT Activity Assay. Finally, we compared the performance of the DA-enabled assay with commonly used methods, which included the dissolved oxygen sensor, spectrophotometric assay (240 nm), ammonium molybdate method, $Ti(SO_4)_2$ method, $KMnO_4$ method, and ferrous oxidation in xylenol orange (FOX) assay. The activities of natural CAT and four representative CAT-like nanozymes (*i.e.*, Pt, PB, CeO_2, and FeNC) were detected for comparison (See SI Figures S26–S31 and associated discussion). In addition, HRP-based assays and the Eu^{3+}-tetracycline (Tc) method were introduced as well (see SI Figure S32 and associated discussion).

All methods mentioned above and our assay are summarized in SI Table S3, with their detected substance, type of determination, main sample requirement, and proper concentration of H_2O_2. Their objective evaluations based on sensitivity, specificity, versatility, and stability (or reproducibility) are shown in Figure 3.

In general, the sensitivity of the CAT activity assay is correlated with the concentration range of H_2O_2. For example, the FOX assay, HRP-based assays, and Eu^{3+}-Tc method are commonly used to detect trace amounts of H_2O_2 (usually at the micromolar level); thus, they have quite high sensitivity (Figure 3g–i). Our DA-enabled assay in this work possesses high sensitivity due to the sensitive response of DA toward oxygen (Figure 3a). Meanwhile, the concentration range of H_2O_2 is much larger than common methods.

The specificity and versatility of the assay are related to the anti-interfering capability and sensitivity. The spectrophotometric assay is not conveniently applicable to complex samples with strong inherent absorbance at 240 nm (Figure 3c). In typical colorimetric methods, H_2O_2 can specifically react with the substrate, followed by color formation or color fading. These methods usually have good specificity toward H_2O_2 but low versatility for different samples because of poor sensitivity (Figure 3d–f,i). FOX and HRP-based assays are not suitable for nanozymes displaying both CAT-like and POD- (or OXD-) like activities. False-positive results will interfere with the determination otherwise (Figure 3g,h). The fluorescence in the Eu^{3+}-Tc method is strongly quenched by phosphate and Cu^{2+}, and weakly affected by molecular oxygen in the solution, which

https://doi.org/10.1021/acs.analchem.2c00804
Anal. Chem. 2022, 94, 10636−10642

limits the application in practice (Figure 3i).[26] Although the DA-enabled assay can monitor the generated oxygen with good specificity, H_2O_2-driven peroxidation of DA may interfere with the assay for CAT activity. The $A_{405\ nm}/A_{480\ nm}$ value we defined in this work could be a measurement index to determine CAT-like or POD-like selectivity. Thus, moderate (or high) specificity is also given toward this assay, which is universal for diverse types of samples (Figure 3a).

The most common methods we mentioned above have good stability (or reproducibility), especially colorimetric methods. For the dissolved oxygen sensor and spectrophotometric assay, the determination is greatly affected by the tested samples and the concentration of H_2O_2, causing obvious variation in the measurements (Figure 3b,c). The DA-enabled assay is a typical colorimetric method with a signal-on response, presenting good stability (or reproducibility).

Clearly, compared with other methods, our DA-enabled assay showed all-round advantages in sensitivity, specificity, versatility, and stability (or reproducibility) for sensing the activity of CAT and particularly CAT-like nanozymes.

Challenges and Opportunities of the Assay. First, we evaluated the adhesive effect caused by the formation of PDA. The concentration of catalysts and the reaction time were the key factors, controlling the dispersive growth of PDA from small islands to connective layers. When the catalyst (such as $LaNiO_3$ nanozyme) was used with a fairly high concentration (200 μg/mL), an obvious PDA shell could form on the surface of $LaNiO_3$ (SI Figure S33a,b), which would attenuate the catalytic activity (SI Figure S33c). Thus, a lower concentration of catalysts should be used for the activity assay, otherwise the catalytic activity would be severely affected or even lost by PDA. Furthermore, reduced reaction time could also minimize the interference of PDA adhesion (see SI Figure S34 and associated discussion). In addition, other potential interferents toward this assay were investigated, including common metal ions, biomolecules, and enzymes (see SI Figures S35−S36 and associated discussion). The results indicated that the interferences toward the assay would be properly negligible.

The DA-enabled assay in this work presented all-round advantages in sensitivity, specificity, and versatility, directly enlarging its range of application in practice. For the emerging area, nanozymes, such a universal assay would promote the formulation of measurement criteria for CAT-like nanozymes. This would facilitate rapid screening and rational design of nanozymes with high efficiency, which could be more effective in biomedical applications.

With regard to the determination of natural CAT, it is reasonable to develop a systematic evaluation of the relative content of CAT in various animal or plant tissues using the DA-enabled assay. Furthermore, this assay provides an alternative and better method to determine salivary CAT activity than conventional spectrophotometric assays. According to previous studies, the average level of salivary CAT was higher in periodontal patients and type I diabetic patients but lower in elderly patients with dementia.[25,27,28] Meanwhile, the collection of saliva is noninvasive and very acceptable to adults even children.[29] Therefore, our assay has the potential to reflect biochemical indexes and further assess physiological status based on the enlargement of the sample size.

In addition, the DA-enabled assay can be converted into commercial CAT activity assay kits. The high quality of the assay kits will bring benefits to routine research or examinations in laboratories, hospitals, and testing institutions. For further product upgrades, portable test strips for CAT activity can be developed for user-friendliness in the future. Thus, this assay not only advances the development of new CAT mimics but also finds broader prospects for applications in various fields.

CONCLUSION

In summary, a DA-based universal assay to detect CAT (or CAT-like) activity by monitoring the generated oxygen was developed in this work. The assay is based on the oxygen-sensitive and H_2O_2-inhibitory polymerization of DA. With this assay, we analyzed diverse types of samples such as natural CAT, CAT-like nanozymes, animal tissues, and human saliva. Importantly, we addressed the limitations of the current assay and emphasized the advantages when testing diverse samples. Compared with common methods, this assay presents all-round advantages in sensitivity, specificity, and versatility, facilitating the formulation of measurement criteria for CAT and CAT-like nanozymes. Given the importance of natural CAT and the rapid development of CAT-like nanozymes, this assay will not only advance the development of new CAT mimics but also find broader applications in various samples, such as plant and patient tissues.

ASSOCIATED CONTENT

Supporting Information

The Supporting Information is available free of charge at https://pubs.acs.org/doi/10.1021/acs.analchem.2c00804.

Additional experimental details, materials, methods, Figures S1−S36, and Tables S1−S3 (PDF)

AUTHOR INFORMATION

Corresponding Authors

Hui Wei − *Department of Biomedical Engineering, College of Engineering and Applied Sciences, Nanjing National Laboratory of Microstructures, Jiangsu Key Laboratory of Artificial Functional Materials, Nanjing University, Nanjing, Jiangsu 210023, China; State Key Laboratory of Analytical Chemistry for Life Science, School of Chemistry and Chemical Engineering, Chemistry and Biomedicine Innovation Center (ChemBIC), Nanjing University, Nanjing, Jiangsu 210023, China*; orcid.org/0000-0003-0870-7142; Email: weihui@nju.edu.cn

Sheng Zhao − *Department of Biomedical Engineering, College of Engineering and Applied Sciences, Nanjing National Laboratory of Microstructures, Jiangsu Key Laboratory of Artificial Functional Materials, Nanjing University, Nanjing, Jiangsu 210023, China*; Email: dg1634033@smail.nju.edu.cn

Authors

Anqi Lin − *Department of Biomedical Engineering, College of Engineering and Applied Sciences, Nanjing National Laboratory of Microstructures, Jiangsu Key Laboratory of Artificial Functional Materials, Nanjing University, Nanjing, Jiangsu 210023, China*

Quanyi Liu − *State Key Laboratory of Electroanalytical Chemistry, Changchun Institute of Applied Chemistry, Chinese Academy of Sciences, Changchun, Jilin 130022, China; University of Science and Technology of China, Hefei, Anhui 230026, China*

https://doi.org/10.1021/acs.analchem.2c00804
Anal. Chem. 2022, 94, 10636−10642

Yihong Zhang − *Department of Biomedical Engineering, College of Engineering and Applied Sciences, Nanjing National Laboratory of Microstructures, Jiangsu Key Laboratory of Artificial Functional Materials, Nanjing University, Nanjing, Jiangsu 210023, China*

Quan Wang − *Department of Biomedical Engineering, College of Engineering and Applied Sciences, Nanjing National Laboratory of Microstructures, Jiangsu Key Laboratory of Artificial Functional Materials, Nanjing University, Nanjing, Jiangsu 210023, China*

Sirong Li − *Department of Biomedical Engineering, College of Engineering and Applied Sciences, Nanjing National Laboratory of Microstructures, Jiangsu Key Laboratory of Artificial Functional Materials, Nanjing University, Nanjing, Jiangsu 210023, China*

Bijun Zhu − *Department of Cariology and Endodontics, Nanjing Stomatological Hospital, Medical School of Nanjing University, Nanjing, Jiangsu 210093, China*

Leiying Miao − *Department of Cariology and Endodontics, Nanjing Stomatological Hospital, Medical School of Nanjing University, Nanjing, Jiangsu 210093, China;* orcid.org/0000-0001-6915-8218

Yan Du − *State Key Laboratory of Electroanalytical Chemistry, Changchun Institute of Applied Chemistry, Chinese Academy of Sciences, Changchun, Jilin 130022, China; University of Science and Technology of China, Hefei, Anhui 230026, China;* orcid.org/0000-0003-3197-7204

Complete contact information is available at: https://pubs.acs.org/10.1021/acs.analchem.2c00804

Author Contributions

A.L. and S.Z. designed the study. H.W. guided the study. A.L. performed the *in vitro* study and analyzed the data. S.Z. performed the *ex vivo* study and analyzed the data. A.L., S.Z., Q.L., Y.Z., and Q.W. synthesized the nanomaterials used in this work. Q.L., Q.W., S.L., B.Z., L.M., and Y.D. assisted with data analysis. The manuscript was written through the contributions of all authors. All authors have approved the final version of the manuscript.

Funding

This work was supported by the National Key R&D Program of China (2019YFA0709200 and 2021YFF1200700), the National Natural Science Foundation of China (21874067 and 21722503), the CAS Interdisciplinary Innovation Team (JCTD-2020−08), the PAPD Program, Fundamental Research Funds for the Central Universities (021314380195), and Postgraduate Research & Practice Innovation Program of Jiangsu Province (KYCX22_0133).

Notes

The authors declare the following competing financial interest(s): Patent application is in progress.

■ ACKNOWLEDGMENTS

We thank Yifeng Xiong for the assistance of the TOC graphic and Chenxin Zhu for the assistance of TEM images.

■ REFERENCES

(1) Guan, L.; Scandalios, J. G. *Proc. Natl. Acad. Sci. U.S.A.* **1995**, *92*, 5930−5934.
(2) Mueller, S.; Riedel, H.-D.; Stremmel, W. *Anal. Biochem.* **1997**, *245*, 55−60.
(3) Shangari, N.; O'Brien, P. J. *Curr. Protoc. Toxicol.* **2006**, 7.7.1−7.7.16.
(4) Fransen, M.; Nordgren, M.; Wang, B.; Apanasets, O. *Biochim. Biophys. Acta* **2012**, *1822*, 1363−1373.
(5) Glorieux, C.; Calderon, P. B. *Biol. Chem.* **2017**, *398*, 1095−1108.
(6) Wu, J.; Wang, X.; Wang, Q.; Lou, Z.; Li, S.; Zhu, Y.; Qin, L.; Wei, H. *Chem. Soc. Rev.* **2019**, *48*, 1004−1076.
(7) Huang, Y.; Ren, J.; Qu, X. *Chem. Rev.* **2019**, *119*, 4357−4412.
(8) Jiang, D.; Ni, D.; Rosenkrans, Z. T.; Huang, P.; Yan, X.; Cai, W. *Chem. Soc. Rev.* **2019**, *48*, 3683−3704.
(9) Zhang, R.; Yan, X.; Fan, K. *Acc. Mater. Res.* **2021**, *2*, 534−547.
(10) Tang, G.; He, J.; Liu, J.; Yan, X.; Fan, K. *Exploration* **2021**, *1*, 75−89.
(11) Singh, N.; Savanur, M. A.; Srivastava, S.; D'Silva, P.; Mugesh, G. *Angew. Chem., Int. Ed.* **2017**, *56*, 14267−14271.
(12) Soh, M.; Kang, D. W.; Jeong, H. G.; Kim, D.; Kim, D. Y.; Yang, W.; Song, C.; Baik, S.; Choi, I. Y.; Ki, S. K.; Kwon, H. J.; Kim, T.; Kim, C. K.; Lee, S. H.; Hyeon, T. *Angew. Chem., Int. Ed.* **2017**, *56*, 11399−11403.
(13) He, L.; Ni, Q.; Mu, J.; Fan, W.; Liu, L.; Wang, Z.; Li, L.; Tang, W.; Liu, Y.; Cheng, Y.; Tang, L.; Yang, Z.; Liu, Y.; Zou, J.; Yang, W.; Jacobson, O.; Zhang, F.; Huang, P.; Chen, X. *J. Am. Chem. Soc.* **2020**, *142*, 6822−6832.
(14) Zhang, Y.; Wang, X.; Chu, C.; Zhou, Z.; Chen, B.; Pang, X.; Lin, G.; Lin, H.; Guo, Y.; Ren, E.; Lv, P.; Shi, Y.; Zheng, Q.; Yan, X.; Chen, X.; Liu, G. *Nat. Commun.* **2020**, *11*, 5421.
(15) Rhee, S. G.; Chang, T. S.; Jeong, W.; Kang, D. *Mol. Cells* **2010**, *29*, 539−549.
(16) Miller, E. W.; Tulyathan, O.; Isacoff, E. Y.; Chang, C. J. *Nat. Chem. Biol.* **2007**, *3*, 263−267.
(17) Song, Y.; Zhang, Y.; Bernard, P. E.; Reuben, J. M.; Ueno, N. T.; Arlinghaus, R. B.; Zu, Y.; Qin, L. *Nat. Commun.* **2012**, *3*, 1283.
(18) Zhu, Z.; Guan, Z.; Liu, D.; Jia, S.; Li, J.; Lei, Z.; Lin, S.; Ji, T.; Tian, Z.; Yang, C. J. *Angew. Chem., Int. Ed.* **2015**, *54*, 10448−10453.
(19) Lee, H.; Dellatore, S. M.; Miller, W. M.; Messersmith, P. B. *Science* **2007**, *318*, 426−430.
(20) Li, J.; Baird, M. A.; Davis, M. A.; Tai, W.; Zweifel, L. S.; Adams Waldorf, K. M.; Gale, M., Jr.; Rajagopal, L.; Pierce, R. H.; Gao, X. *Nat. Biomed. Eng.* **2017**, *1*, 0082.
(21) Napolitano, A.; Crescenzi, O.; Pezzella, A.; Prota, G. *J. Med. Chem.* **1995**, *38*, 917−922.
(22) Li, J.; Wang, T.; Kirtane, A. R.; Shi, Y.; Jones, A.; Moussa, Z.; Lopes, A.; Collins, J.; Tamang, S. M.; Hess, K.; Shakur, R.; Karandikar, P.; Lee, J. S.; Huang, H.-W.; Hayward, A.; Traverso, G. *Sci. Transl. Med.* **2020**, *12*, No. eabc0441.
(23) Chen, W. H.; Vazquez-Gonzalez, M.; Kozell, A.; Cecconello, A.; Willner, I. *Small* **2018**, *14*, 1703149.
(24) Ibrahim, W.; Lee, U.-S.; Yen, H.-C.; Clair, D. K. S.; Chow, C. K. *Free Radical Bio. Med.* **2000**, *28*, 397−402.
(25) Kraus, F. W.; Perry, W. I.; Nickerson, J. F. *Or. Surg. Or. Med. Or. Pa.* **1958**, *11*, 95−102.
(26) Wu, M.; Lin, Z.; Wolfbeis, O. S. *Anal. Biochem.* **2003**, *320*, 129−135.
(27) Choromanska, M.; Klimiuk, A.; Kostecka-Sochon, P.; Wilczynska, K.; Kwiatkowski, M.; Okuniewska, N.; Waszkiewicz, N.; Zalewska, A.; Maciejczyk, M. *Int. J. Mol. Sci.* **2017**, *18*, 2205.
(28) Maleki, S.; Falsafi, P.; Pakdel, F.; Eslami, H.; Ahari, U.; Ghanizadeh, M.; Pouralibaba, F. *Biomed. Pharmacol. J.* **2016**, *9*, 463−468.
(29) Zalewska, A.; Kossakowska, A.; Taranta-Janusz, K.; Zieba, S.; Fejfer, K.; Salamonowicz, M.; Kostecka-Sochon, P.; Wasilewska, A.; Maciejczyk, M. *J. Clin. Med.* **2020**, *9*, 548.